Modulation of calreticulin expression reveals a novel exosome-mediated mechanism of Z variant α_1-antitrypsin disposal

Received for publication, October 4, 2018, and in revised form, February 26, 2019 Published, Papers in Press, March 4, 2019, DOI 10.1074/jbc.RA118.006142

Nazli Khodayari[‡], Regina Oshins[‡], Abdel A. Alli[§], Kubra M. Tuna[§], L. Shannon Holliday[¶], Karina Krotova[‖], and Mark Brantly[‡1]

From the [‡]Division of Pulmonary, Critical Care and Sleep Medicine, Department of Medicine, the [§]Department of Physiology and Functional Genomics, College of Medicine, and the [¶]Department of Orthodontics, College of Dentistry, University of Florida, Gainesville, Florida 32610 and the [‖]Hormel Institute, University of Minnesota, Austin, Minnesota 55912

Edited by George N. DeMartino

α_1-Antitrypsin deficiency (AATD) is an inherited disease characterized by emphysema and liver disease. AATD is most often caused by a single amino acid substitution at position 342 in the mature protein, resulting in the Z mutation of the AAT gene (ZAAT). This substitution is associated with misfolding and accumulation of ZAAT in the endoplasmic reticulum (ER) of hepatocytes, causing a toxic gain of function. ERdj3 is an ER luminal DnaJ homologue, which, along with calreticulin, directly interacts with misfolded ZAAT. We hypothesize that depletion of each of these chaperones will change the fate of ZAAT polymers. Our study demonstrates that calreticulin modulation reveals a novel ZAAT degradation mechanism mediated by exosomes. Using human PiZZ hepatocytes and K42, a mouse calreticulin-deficient fibroblast cell line, our results show ERdj3 and calreticulin directly interact with ZAAT in PiZZ hepatocytes. Silencing calreticulin induces calcium independent ZAAT–ERdj3 secretion through the exosome pathway. This co-secretion decreases ZAAT aggregates within the ER of hepatocytes. We demonstrate that calreticulin has an inhibitory effect on exosome-mediated ZAAT–ERdj3 secretion. This is a novel ZAAT degradation process that involves a DnaJ homologue chaperone bound to ZAAT. In this context, calreticulin modulation may eliminate the toxic gain of function associated with aggregation of ZAAT in lung and liver, thus providing a potential new therapeutic approach to the treatment of AATD-related liver disease.

α_1-Antitrypsin deficiency (AATD)-associated[2] liver disease is caused by accumulation of misfolded α_1-antitrypsin (AAT) in the endoplasmic reticulum (ER) of hepatocytes (1). The presentation of AATD-associated liver disease ranges from hepatitis and cirrhosis to fulminant hepatic failure. The overall risk of liver disease is 40% in PiZZ adults and 5% in PiZZ children (2). Late-stage liver disease can only be treated by liver transplantation (2, 3).

AAT, a 52-kDa glycoprotein encoded by the SERPINA1 gene and mainly produced by hepatocytes, is the most prevalent serine protease inhibitor in human plasma. AATD is a conformational disorder associated with mutations of the SERPINA1 gene. The most prevalent disease-related mutation is the Z form, which results in misfolding and accumulation of AAT within the ER of hepatocytes, causing a toxic gain of function (4). Chaperones involved in ZAAT degradation include calnexin, calreticulin (CALR), PDI, ERdj3, GRP78/BiP, and EDEM1 (5, 6). ERdj3 is one of the soluble ER-associated Hsp40 families, which is highly expressed in the liver. Recently we have shown that ERdj3, along with calreticulin, is a part of the ZAAT trafficking network. We reported that depleting ERdj3 increased the rate of ZAAT degradation in hepatocytes by redirecting ZAAT proteasome-dependent degradation by autophagosome formation (6).

It has been shown that ZAAT is eliminated from the secretory pathway by ER-associated degradation (7), but a small amount is secreted into the blood and is able to inhibit neutrophil elastase activity with a reduced capacity compared with M variant AAT (MAAT) (8). How misfolded proteins are released into the extracellular environment remains under debate. Unconventional secretion pathway of accumulated misfolded proteins within the cytoplasm caused by overloading of the proteasome has recently been proposed to describe misfolding-associated secretion pathways (9).

A few reports suggest that some misfolded proteins might secrete to the extracellular space using an exosome pathway (10, 11), (12, 13). Exosomes are a subpopulation of extracellular vesicles, derived from the endolysosomal pathway, ranging in size from 30 to 150 nm in diameter (14). They are highly mul-

This work was supported by a grant from the Alpha-1 Foundation and National Institutes of Health National Center for Advancing Translational Sciences Grant UL1 TR000064. The authors declare that they have no conflicts of interest with the contents of this article. The content is solely the responsibility of the authors and does not necessarily represent the official views of the National Institutes of Health.

This article contains Figs. S1 and S2.

[1] To whom correspondence should be addressed: Division of Pulmonary, Critical Care and Sleep Medicine, University of Florida, College of Medicine, 1600 SW Archer Rd., Rm. M454A, JHMHC, P.O. Box 100225, Gainesville, FL 32610. Tel.: 352-273-8735; Fax: 352-273-9154; E-mail: mbrantly@ufl.edu.

[2] The abbreviations used are: AATD, AAT deficiency; AAT, α_1-antitrypsin; ZAAT, Z variant of AAT; ER, endoplasmic reticulum; CALR, calreticulin; siCALR, small interfering RNA against calreticulin; NT, nontargeted; EC, extracellular; IC, intracellular; MAAT, M variant AAT; RIPA, radioimmunoprecipitation assay; NTA, nano tracking analysis; EV, extracellular vesicle; MVB, multivesicular body; IP, immunoprecipitation; TEA_AC, triethylammonium acetate; KO, knockout.

tifunctional vesicles (15), containing different proteins that are involved in specific cell functions (16). There is a growing body of evidence suggesting that exosomes are involved in physiological and pathological processes, and new studies are focused on their clinical application (14).

In this study, we provide direct evidence that calreticulin depletion may lead to secretion of ZAAT in a complex form with ERdj3 through an exosome-mediated pathway. Packaging misfolded proteins in an enclosed membrane compartment may offer protection against ZAAT-mediated toxic gain of function in hepatocytes that accumulate misfolded ZAAT. Taken together, our study suggests that exosomes, when proteasomal function is impaired, might contribute to the off-site degradation of misfolded proteins. Further study of this phenomenon may lead to new therapeutic approaches in AAT aggregation-induced cell toxicity.

Results

Calreticulin depletion increases the extracellular level of ZAAT and ERdj3

It has been shown that ER stress can lead to secretion of ERdj3 into the media. Secreted ERdj3 can bind misfolded substrates and prevent their extracellular aggregation (17). Our previous studies revealed that ERdj3 competes with calreticulin when binding to ZAAT and delays ZAAT degradation (6). We extended these experiments using small interfering RNA against calreticulin (siCALR) to follow the ZAAT trafficking pathway. AAT knockout Huh 7.5 cells were transfected with nontargeted (NT) siRNA or siCALR followed by ZAAT transient transfection. Calreticulin silencing was confirmed by quantitative PCR showing 90% silencing efficiency (Fig. 1*C*). Conditioned media (extracellular (EC)) and lysate (intracellular (IC)) were analyzed for AAT, ERdj3, and major chaperones within the ER by their mobility on SDS gels. Actin was examined as loading control (Fig. 1*A*). We found that knockdown of endogenous calreticulin increases ZAAT and ERdj3 secretion into the medium, whereas other chaperones were expressed at similar levels (*lanes 6* and *8*). The observation that ERdj3 and ZAAT are more abundant in the conditioned media led us to ask whether calreticulin knockdown triggers increased mRNA expression level of ZAAT and ERdj3. We performed quantitative PCR analysis on NT siRNA- and siCALR-treated Huh 7.5 cells transfected with ZAAT or MAAT expression plasmids. We found a 2-fold increase in ERdj3 mRNA levels (Fig. 1*B*), which may explain the constant level of ERdj3 within the cells treated with siCALR and the comparatively higher level of ERdj3 within the media. It is important to point out that no toxicity (Fig. S1*A*) was detected after calreticulin depletion, and siCALR did not induce a strong UPR response, just a small rise in a select few proteins associated with ER-associated degradation (Fig. S1*B*) consistent with previous reports (18). To evaluate the level of ZAAT secretion, a similar experiment was performed using ^{35}S pulse–chase analysis. Silencing calreticulin considerably enhances the level of ZAAT secretion in a 40-min chase period in ZAAT-expressing Huh 7.5 cells (Fig. 1*D*). The ZAAT secretion levels started at the 2-min time point with a near 2-fold increase consistently at all time points (Fig. 1, *D* and *E*, second lane).

ERdj3 is co-secreted with ZAAT as a protein complex

ERdj3 may regulate ZAAT cellular trafficking through a direct interaction (6). To test for a possible interaction between ZAAT and ERdj3 in the media, a co-immunoprecipitation study was performed on the conditioned media, as well as the cell lysate in NT siRNA- and siCALR-treated Huh 7.5 cells transfected with ZAAT or MAAT expression plasmids (Fig. 2, *A* and *B*). We found that under steady-state conditions, secreted ERdj3 in the conditioned media is bound to AAT (*Lane* 2, both immunoprecipitation panels). The same experiment was performed for WT K41 and calreticulin-deficient K42 cell lines (19) transfected with ZAAT plasmid. The results showed elevated ZAAT and ERdj3 in the conditioned media consistent with results from the Huh 7.5 cell line (Fig. 2, *A* and *B*). To characterize the subcellular localization of the ZAAT–ERdj3 complex within the cells, we performed density gradient isolation of cellular proteins from the ZAAT-expressing cells treated with NT siRNA or siCALR. Treatment with siCALR resulted in migration of different glycosylated forms of ZAAT from the ER to lighter fractions along with ERdj3, CD63, and CD81 (*lanes 2*, *3*, *5*, and *6*). BiP and calnexin were loaded to demonstrate the integrity of the ER in the presence of siCALR (*lanes 7* and *8*) (Fig. 2, *C* and *D*). Quantified integrated density bars illustrate the effect of siCALR on subcellular localization of ZAAT and ERdj3 (Fig. 2*D*). Co-immunoprecipitation analysis of fractions pooled in groups of three showed that in the NT siRNA-treated cells, there are ZAAT–ERdj3 complexes located in the fractions 7–10 that co-localize with the ER markers such as BiP and calnexin. CALR depletion leads to translocation of the ZAAT–ERdj3 complex through the lighter fractions that are closer to the cell membrane (Fig. 2*E*). The intracellular level of exogenous ZAAT in K41 and K42 cell lines shown by comparing the integrated density of the total red fluorescent measurements from four different 10× images/sample revealed a considerable reduction in ZAAT staining in K42 cells compared with the WT control (Fig. 2*F*).

Unconventional secretion of ZAAT–ERdj3 complexes as a result of the ER to Golgi blockade

MAAT undergoes ER glycosylation and transport to the Golgi complex by entrance into coat protein complex II vesicles (7). It is thought that ZAAT is also transported through the Golgi and secreted into extracellular space in lesser amounts compared with MAAT (20). ERdj3, an intracellular protein that can be secreted into the extracellular space, lacks a signal sequence for classical secretion (21). Therefore, we asked how ZAAT–ERdj3 gains access to the plasma membrane. To determine the secretion pathway of ZAAT–ERdj3, brefeldin A, an inhibitor of the classical ER/Golgi secretion pathway, was applied to the NT siRNA- and siCALR-treated Huh 7.5 cells transfected with ZAAT expression plasmid. The result showed that ZAAT–ERdj3 secretion is insensitive to the treatment of cells with brefeldin A (Fig. 3, *A*–*C*). Treatment with brefeldin A causes accumulation of ZAAT within the cells in normal conditions, whereas siCALR treatment leads to clearance of the IC

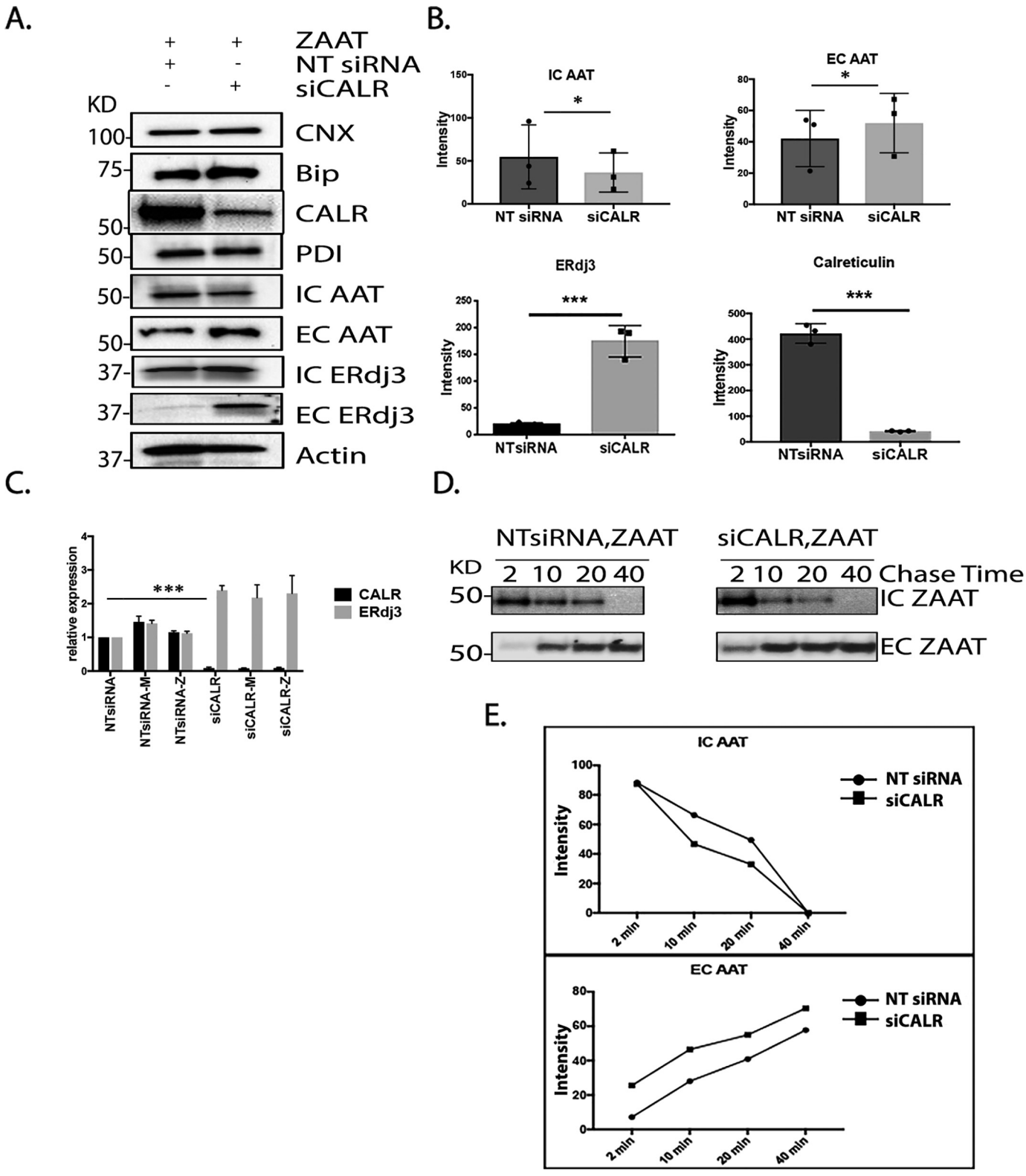

Figure 1. Calreticulin depletion increases the extracellular level of ZAAT and ERdj3. *A*, NT siRNA or siCALR was introduced 24 h before ZAAT transfection to AAT KO Huh 7.5 cells. Western blotting analysis shows the expression level of main chaperones within the ER, as well as IC and elevated EC level of ZAAT and ERdj3. Actin was examined as a loading control. *CNX*, calnexin; *PDI*, protein disulfide-isomerase. *B*, quantification of the band intensities of IC AAT, EC AAT, EC ERdj3, and calreticulin fractions. Differences were assessed by two-tailed *t* test analysis (*, $p < 0.05$; ***, $p < 0.005$). *C*, RNA expression level of calreticulin and ERdj3 in the presence and absence of siCALR in Huh7.5 cells expressing ZAAT and MAAT. *D*, IC and EC level of ZAAT from NT siRNA and siCALR-treated cells were shown during 40 min of pulse–chase radiolabeling. *E*, IC and EC ZAAT quantified density bars during 40-min chase period.

ZAAT and ERdj3. siCALR treatment also leads to an increase in secretion level of both proteins in the presence and absence of brefeldin A treatment (*lanes* 3 and 5), whereas secretion of MAAT was completely inhibited under the same conditions (Fig. 3*D*). Density gradient isolation of cellular proteins from the ZAAT-expressing cells treated with NT siRNA or siCALR in the presence of brefeldin A treatment confirmed migration of ZAAT from ER to the lighter fraction along with ERdj3 (Fig. 3, *E* and *F*). Immuno-

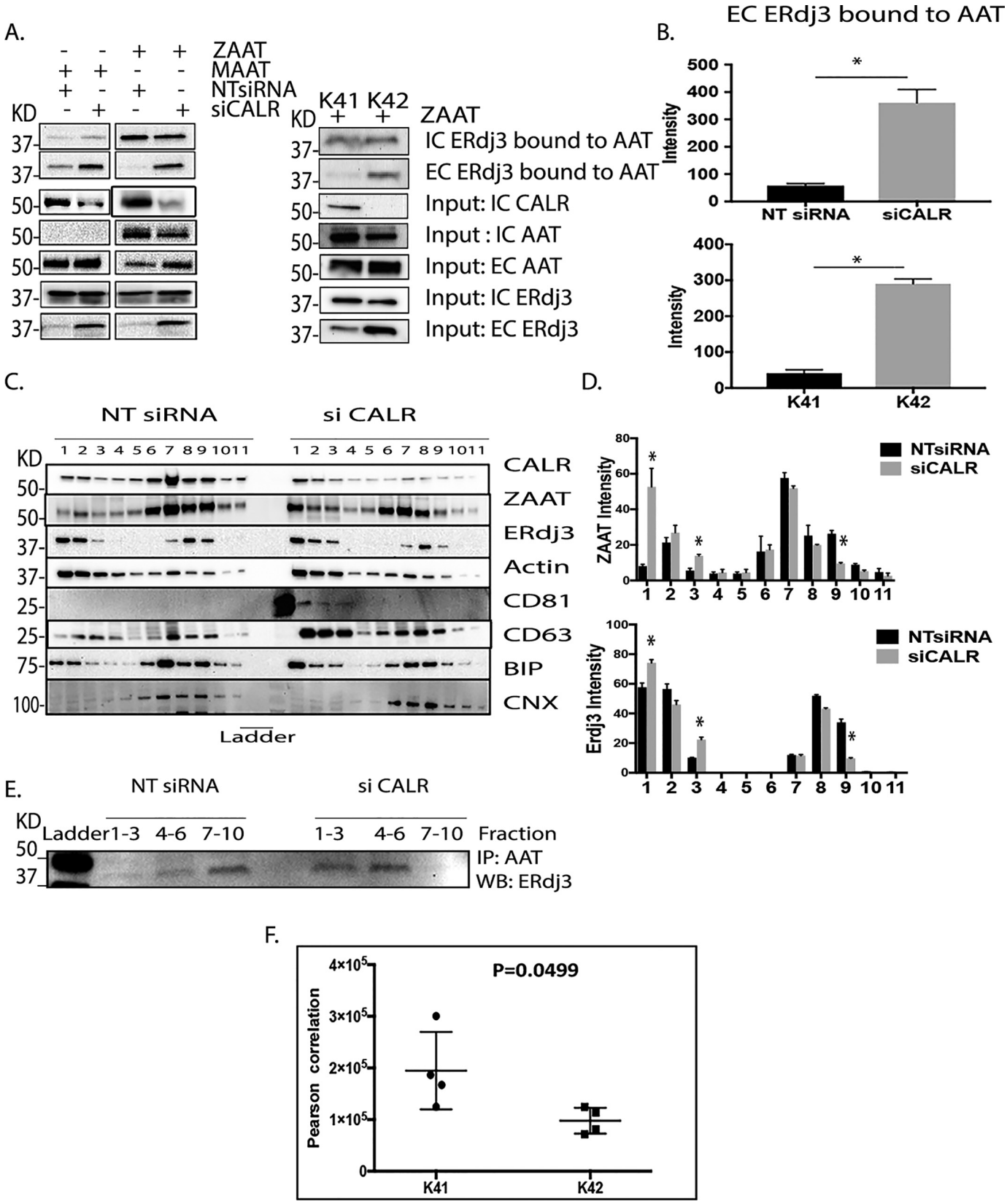

fluorescent microscopy analysis showed that siCALR treatment in the presence of brefeldin A causes a more vesicular localization of ZAAT in *green* and ERdj3 in *red* (Fig. 3*G*, *lanes 2* and *4*) compared with the NT siRNA treatment (*lanes 1* and *3*). These results suggest ZAAT–ERdj3 is secreted via a different pathway from the classical ER/Golgi secretion pathway.

ZAAT–ERdj3 release from cells in association with exosomes

Based on previous reports, the Hsp40 family is secreted and transmitted intracellularly by exosomes (21). To further investigate the secretion pathway of ZAAT–ERdj3 complex released from cells, we sought for membrane-enclosed compartments containing ZAAT and ERdj3 in the medium. Conditioned media were subjected to immunoprecipitation for AAT with and without RIPA buffer or Nonidet P-40 (Fig. 4*A*). The results showed that a significant portion of AAT is not accessible to the antibody without detergent, which agrees with the presence of a significant fraction of AAT in membrane-enclosed compartments. To assess whether an exosome-mediated pathway could be involved in the secretion of the complex, exosome isolation and purification were performed following an established centrifugation protocol (22). Isolated exosomes from the conditioned media of AAT knockout Huh 7.5 cells, K41 and K42 mouse fibroblast cell lines transfected with ZAAT (Fig. S2*A*), or ZAAT after NT siRNA or siCALR treatment in Huh 7.5 cells were separated. EM experiments confirmed the morphological characteristics of small vesicles with a diameter of 100–150 nm (Fig. 4*B*). The size and concentration of the exosomes was assessed using NTA analysis, which showed single population of exosomes in the exosome pellet derived from NT siRNA-treated ZAAT-expressing hepatocytes, compared with two distinct population of exosomes in siCALR-treated ZAAT-expressing hepatocytes (Fig. 4*C*). Western blotting of isolated exosomal fractions from NT siRNA- and siCALR-treated samples demonstrate the exosome marker proteins flotilin-1, annexin A2, and Hsp70. AAT and ERdj3 also were detected in NT siRNA- and siCALR-treated samples with a significant increase in exosome fraction derived from siCALR-treated cells (Fig. 4, *D* and *E*). The pellet from 40 ml of conditioned media from siCALR-treated AAT knockout cells transfected with ZAAT was fractionated by Opti-Prep density gradient centrifugation to confirm co-localization of AAT and ERdj3 within the exosome fraction, as well as to rule out other protein aggregates and contaminants. Other groups have previously shown that sucrose density gradients allow separation of an exosome subpopulation (23, 24). When we loaded the exosome pellet resuspended in 300 μl of PBS on top of the sucrose gradient followed by ultracentrifugation for 18 h, we detected the clear bands of ERdj3 and ZAAT in the lower density fractions of 1.069 and 1.079 g/ml with exosomal marker proteins CD63, ALIX, and TSG101 (Fig. 4*F*). These observations are consistent with data obtained from NTA analysis, which showed a separate population of exosomes in siCALR-treated samples that was smaller in size (Fig. 4*C*).

ZAAT–ERdj3 is secreted through endosomal pathway

To examine whether early endosomes are important for exosome-mediated ZAAT–ERdj3 secretion, we quantified ZAAT and ERdj3 in cells expressing a GFP-Q79L-Rab5 plasmid, a constitutively active Rab5 mutant that develops enlarged cytoplasmic vesicles with many characteristics of early endosomes, including immunoreactivity for Rab5 and transferrin receptor (25). Detecting ERdj3-containing (Fig. 5*A*) and ZAAT-containing (Fig. 5*B*) vesicles in GFP decorated Q79L-Rab5 endosomes in siCALR-treated cells compared with NT siRNA samples by immunofluorescent microscopy suggested that exosome synthesis may occur at this location. To confirm this finding, 20 μM NT siRNA and siCALR were introduced to the AAT KO Huh 7.5 cells 24 h prior to ZAAT transient transfection. 48 h after ZAAT transfection brefeldin A was applied to the cells for 6 h, and then ERdj3, ZAAT, and CD63 were labeled and analyzed using fluorescent microscopy. The results show that in the presence of siCALR both ERdj3 (Fig. 5*C*) and ZAAT (Fig. 5*D*) were co-localized with CD63, a marker that traffics through the endosomal route (26) and is enriched in the large endosomal fraction.

Discussion

In this study, we found that ZAAT is released by cells in a complex with ERdj3 in association with extracellular vesicles (EVs). Extracellular protein misfolding has potentially pathological consequences of secretion of misfolded proteins into the extracellular fluids (27). Extracellular chaperones are known to stabilize misfolded proteins and inhibit their aggregation in addition to delivering them to the cell receptors for internalization and further degradation. This mechanism leads to clearing potentially dangerous aggregates from extracellular spaces (27, 28). ERdj3, a canonical co-chaperone, is known to efficiently secrete to the extracellular space because of ER stress and seems to protect the extracellular environment from potentially toxic

Figure 2. Erdj3 is co-secreted with ZAAT as a protein complex in the absence of calreticulin. *A*, ERdj3 was co-immunoprecipitated with IC and EC MAAT or ZAAT from Huh7.5 cells transfected with NT siRNA or siCALR, as well as K41 and CALR-deficient K42 cells. NT siRNA or siCALR was introduced 24 h before ZAAT or MAAT transfection to AAT KO Huh 7.5 cells. K41 and CALR-deficient K42 cells were transfected with ZAAT plasmid for 48 h. Anti-rabbit AAT antibody was conjugated to protean A Dynabeads and incubated with the cell lysates or conditioned media overnight. After several wash steps, Western blotting was performed using anti-rabbit ERdj3 antibody. *B*, quantification of the band intensities of EC ERdj3 bound to ZAAT in Huh 7.5 and K42 cell line conditioned media. Differences were assessed by two-tailed *t* test analysis. *, $p = 0.013$; **, $p = 0.002$. *C*, density gradient fraction of cellular proteins form a single gel for the ZAAT-expressing Huh7.5 cells treated with NT siRNA or siCALR shows that siCALR treatment results in ZAAT and ERdj3 relocation to the lighter fractions accompanied by CD63 and CD81 exosomal markers. BiP and calnexin were loaded to confirm the integrity of the ER within the treated cells. *D*, quantification of the band intensities of ZAAT and ERdj3 fractions. Differences were assessed by two-tailed *t* test analysis. *, $p < 0.05$. *E*, co-IP of fractions pooled in groups of three shows the movement of the ZAAT–ERdj3 complex from the ER to the lighter fraction. Anti-rabbit AAT antibody was conjugated to Protean A Dynabeads and incubated with the fractions pooled in groups of three overnight. After several wash steps, Western blotting was performed using anti-rabbit ERdj3 antibody. *F*, Pearson correlation coefficients graph for total fluorescent intensity signal from four different images of the ZAAT-expressing K41 and K42 cell lines (10× magnification images) shows the lower level of ZAAT accumulated within the K42 cells compare with the WT K41 cells. K41 and K42 cells were grown on the slides and transfected with ZAAT plasmid for 48 h. ZAAT was labeled with mouse anti-AAT antibody. Total fluorescent intensity signals from four different slides were calculated by Volocity 6.3.

misfolded protein conformations (29). ERdj3 binds misfolded proteins such as ZAAT in the ER of hepatocytes (6, 30). We showed that ERdj3 also binds to calreticulin, the ER-resident lectin chaperone, with the capacity for binding to ZAAT within the ER of hepatocytes (6). Thus, we evaluated the fate of ZAAT in calreticulin depletion circumstances.

Totally unexpected results were obtained upon silencing calreticulin in hepatocytes expressing ZAAT, which were con-

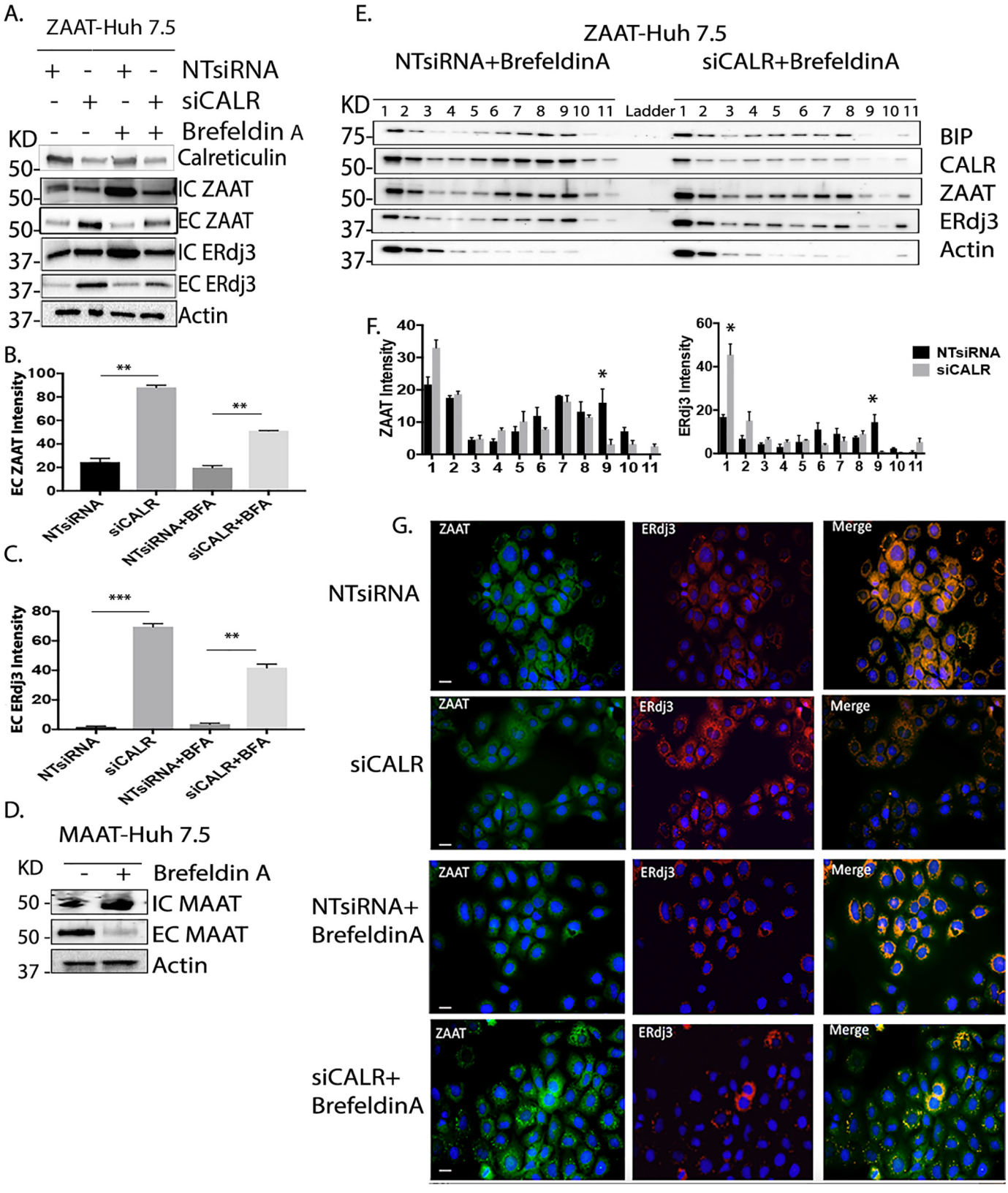

firmed using a calreticulin-deficient mouse fibroblast cell line, K42. In our case ZAAT, a glycoprotein that depends on calreticulin for maturation, appeared as a complex with ERdj3 in the conditioned media in the presence of calreticulin siRNA. ERdj3 binds misfolded protein conformations intracellularly (31) and extracellularly under ER stress conditions (17).

We propose the following mechanism by which calreticulin depletion releases misfolded ZAAT–ERdj3 complexes from the calreticulin/calnexin cycle and allows for retrograde transports of the complex to the cytosol, where they are expected to be degraded by the proteasome. It has been reported that the release of the misfolded glycoprotein from the calreticulin/calnexin cycle results in degradation of the protein (32). Moreover, it has been shown that there is a lag in the ZAAT disposal mechanism, and proteasomal machinery is able to degrade ZAAT when expressed at low levels (33). When the proteasome is not efficiently degrading ZAAT–ERdj3 complexes, they will accumulate in the cytoplasm. ZAAT–ERdj3 accumulation within the cytoplasm results in proteotoxic stress caused by overloading of lysosome and proteasome-mediated degradation machineries. It has been suggested that lysosomal dysfunction or overload may be compensated by exosomal release from the cell (34). Considering the endosomal-lysosomal origin of the exosomes, we can conclude that the excess amount of ZAAT–ERdj3 within the cytoplasm releases in association with EVs. It is reasonable to suggest that when degradation and recycling pathways are overloaded, the misfolded ZAAT accompanied by ERdj3 is routed to the plasma membrane by exosomes.

We now show that off-site degradation of misfolded ZAAT mediated by exosomal secretion is a novel degradation system to diminish ZAAT toxic gain of function in hepatocytes (Fig. 6). Alternatively, ERdj3 works as a co-chaperone to delivering the substrates to the BiP. The data show that ERdj3 co-secretes with unstable BiP substrates when BiP activity is overwhelmed (29). This mechanism challenges extracellular proteostasis during stress situations. In our previous work, we proposed the interaction between calreticulin and ERdj3 in hepatocytes. Because calreticulin depletion leads to co-secretion of ZAAT and ERdj3, we provide evidence that ZAAT–ERdj3 may release from cells because of the lack of available calreticulin within the ER by the same mechanism as BiP. In response to ER stress where calreticulin is not functional, ERdj3 co-secretes with ZAAT to regulate extracellular space proteostasis from ZAAT aggregates. This mechanism can be an extracellular space quality control and reduce the subsequent extracellular aggregation of misfolded ZAAT associated with AATD (20).

This study also uncovers an unconventional pathway that targets misfolded ZAAT for secretion, which includes EVs. In this process, we found that the morphology, size, and protein composition of the EVs containing ZAAT–ERdj3 are like those of exosomes. Exosomes are subpopulations of EVs that were detected based on migration speed in a sucrose gradient (35) and that mediate intracellular transmission of their cargo to regulate various physiological pathways (36, 37). Exosomes are enriched in some common proteins, such as chaperones, TSG101, tetraspanins, and cytoskeletal proteins (38), as well as proteins that are dependent on their cells of origin. The presence of ALIX, CD63, TSG101, and flotilin-1 (39), as well as annexin A1 in the extracellular vesicles containing the ZAAT–ERdj3 complex, is consistent with the association of secreted ZAAT–ERdj3 with exosomes. Flotilin-1, a resident membrane protein of caveolae, is recently shown to be a part of lipid rafts in endosomes. It is also important for endosomal sorting and recycling of specific cargo molecules (40) and was clearly detected on the purified exosomal pellet from conditioned media of the cells. Flotillin-1 predominantly localizes to the plasma membrane and endosomal structures, such as late endosomes and exosomes (41). This idea is strongly supported by the localization of ZAAT–ERdj3 to multivesicular endosomes and exosomes and is consistent with the recent study showing Hsp40 family intercellular transmission contributes to maintenance of extracellular proteostasis via exosomes (21).

We show that exosome-associated ZAAT–ERdj3 secretion is insensitive to brefeldin A in hepatocytes. Hypothetically, despite a few limitations, brefeldin A inhibits protein secretion by limiting Golgi-specific coat proteins involved in maintaining the structural integrity of the Golgi complex. Brefeldin A also negatively regulates membrane transport in the secretory pathway (42). It induces *trans*-Golgi fusion with the ER (43), as well as Golgi fusion with early endosomes and produces a vesicular network (44). Based on our understanding, we suggest the following scenario for the brefeldin A response. The COPII vesicles transfer ZAAT–ERdj3 complexes to the Golgi apparatus. Because of the brefeldin A treatment, the Golgi complexes fuse with early endosomes. The ZAAT–ERdj3 complex anterograde translocates to the Golgi complexes and early endosomes and sorts into exosomes and multivesicular body (MVB) forms. These vesicles are secreted into the extracellular space as MVBs and fuse with the plasma membrane (45).

Accumulation of misfolded ZAAT within hepatocytes is a characteristic of AATD-mediated liver disease; thus, ER clearance of aggregates has been considered as a therapeutic strategy (46). The molecular basis of the ZAAT secretion pathway not only suggests a physiological link between the exosomal secretory pathway and protein degradation machinery but also provides new therapeutic possibilities for protein misfolding diseases such as AATD-associated liver disease.

Figure 3. The effect of brefeldin A on siCALR-mediated noncanonical ZAAT–ERdj3 secretion. *A*, brefeldin A has a minor effect on ZAAT secretion, as well as ERdj3 secretion mediated by siCALR. Actin was loaded as control. *B* and *C*, quantification of the band intensities of EC ZAAT (*B*) and ERdj3 in Huh 7.5 conditioned media (*C*). Differences were assessed by two-tailed *t* test analysis. **, $p = 0.001$; ***, $p = 0.0006$. *D*, lysate and media collected from MAAT expressing Huh 7.5 cell line show that MAAT secretion was completely inhibited by brefeldin A. *E*, single gel, density gradient fractions of cellular proteins in the presence of brefeldin A upon treatment of NT siRNA and siCALR consistently shows relocation of ZAAT and ERdj3 to the lighter fractions in the presence of siCALR. *F*, quantification of the band intensities of IC ZAAT and ERdj3 in Huh 7.5. Differences were assessed by two-tailed *t* test analysis. *, $p < 0.05$. *G*, ZAAT and ERdj3 co-localize together upon siCALR treatment in vesicular compartments. Brefeldin A treatment enhances the vesicular co-localization of ZAAT with ERdj 3. NT siRNA or 20 mM of siCALR was introduced 24 h after ZAAT transfection to AAT KO Huh 7.5 cells. The cells were treated 48 h later with or without brefeldin A for 6 h. ZAAT was labeled with mouse anti-AAT antibody (Alexa 488; *red*) and ERdj3 using rabbit anti-Erdj3 (Alexa 594; *green*). *Scale bars*, 10 μm.

Experimental procedures

Cell lines and cell culture

In-house established human AAT knockout Huh 7.5 and WT (K41) and calreticulin-deficient (K42) mouse embryonic fibroblasts (19), a gift from Dr. M. Michalak (University of Alberta), were maintained in Dulbecco's modified Eagle's medium/F-12 medium (Thermo Scientific) supplemented with 10% fetal bovine serum (VWR, Radnor, PA) or exosome-depleted FBS (System Biosciences, Palo Alto, CA) for exosome purification and 100 μg/ml of Primocin (InvivoGen, San Diego, CA). AAT knockout Huh 7.5 cells were transfected with NT siRNA or siCALR (Life Technologies)

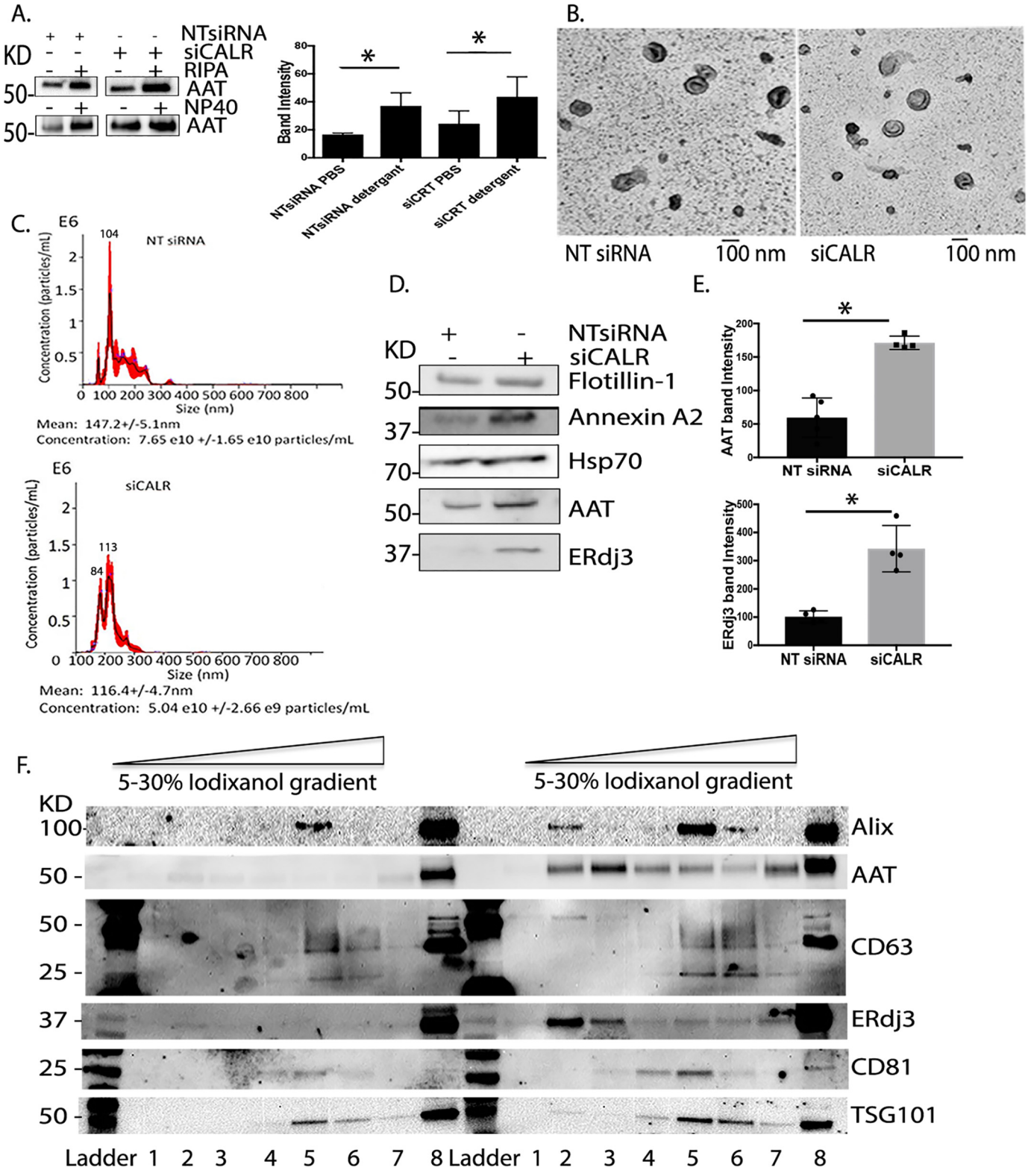

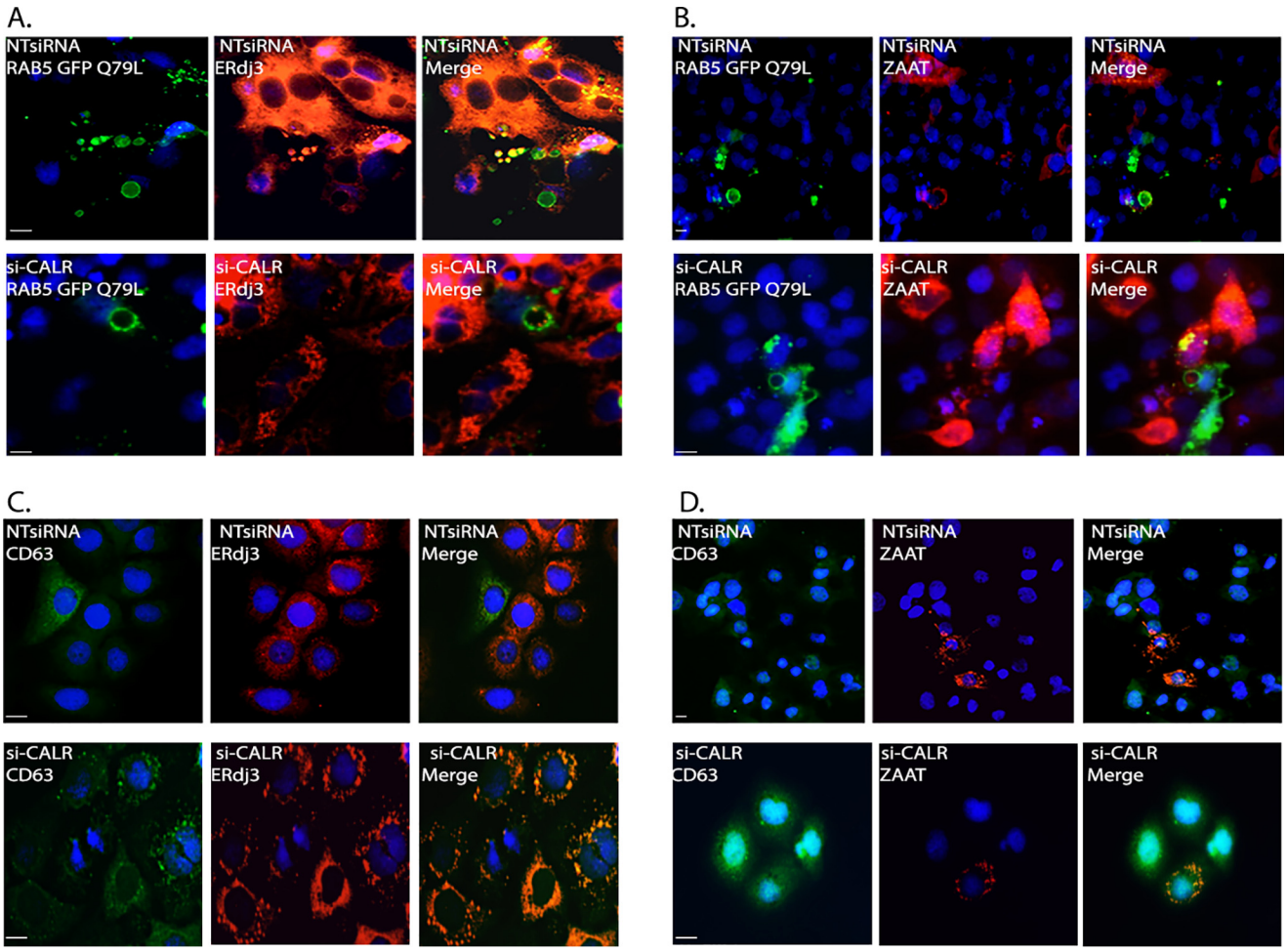

Figure 5. ZAAT–ERdj3 are secreted through endosomal pathway. *A*, immunofluorescent micrographs showing the accumulation of Erdj3 (*bottom row*) inside the lumen of enlarged endosomes outlined by GFP-Q79L-RAB5(Q79L) in CALR-depleted cells. 20 mM of siCALR was introduced 24 h after ZAAT and GFP-Q79L Rab5 co-transfection to AAT KO Huh 7.5 cells. Then 48 h later, ERdj3 was immunoassayed using rabbit anti-Erdj3 (Alexa Flour 594; *red*). *Scale bars*, 10 μm. *B*, immunofluorescent micrographs showing the accumulation of ZAAT (*bottom row*) inside the lumen of enlarged endosomes outlined by GFP-Q79L-RAB5(Q79L) in CALR-depleted cells. ZAAT was labeled using mouse anti-AAT antibody (Alexa Flour 546; *red*). *Scale bars*, 10 μm. *C*, immunofluorescent micrographs showing the co-localization of ERdj3 with CD63 (*bottom row*), an endosomal derived exosome marker. 20 mM of siCALR was introduced 24 h after ZAAT transfection to AAT KO Huh 7.5 cells. Then the cells were treated 48 h later with brefeldin A for 6 h. ERdj3 was immune-labeled using mouse anti-Erdj3 (Alexa Flour 546; *red*). CD63 was immune-labeled using rabbit anti-CD63 antibody (Alexa Flour 488; *green*). *Scale bars*, 10 μm. *D*, immunofluorescent micrographs showing the co-localization of ZAAT with CD63 (*bottom row*), an endosomal derived exosome marker ZAAT was immune-labeled using mouse anti-AAT antibody (Alexa Flour 546; *red*). *Scale bars*, 10 μm.

overnight using Lipofectamin RNAiMAX reagent (Invitrogen) and transfected with pTR2-ZAAT plasmid or pTR2-MAAT and GFP-Q79L-Rab5 from Addgene (Cambridge, MA) using X-tremeGENE HP DNA transfection reagent (Roche Applied Science) 24 h after silencing. Then, 48 h after transfection, the cells were evaluated by Western blotting, co-immunoprecipitation (co-IP), metabolic labeling, or immunofluorescence experiments.

Figure 4. ZAAT–ERdj3 complex release from cells in association with exosomes. *A*, the level of detectable ZAAT within the conditioned media from KO Huh cells transfected with ZAAT plasmid, in the presence and absence of RIPA buffer and Nonidet P-40 shows that a significant portion of ZAAT is not accessible to the antibody without the detergent. The *graph* in the *right panel* shows the band intensities result from the Western blotting experiment in the *left panel*. Differences were assessed by two-tailed *t* test analysis. *, $p < 0.05$. *B*, morphological characterization of exosomes from NT siRNA- and siCALR-treated Huh 7.5 medium by transmission EM. *C*, NanoSight tracking analysis of size and concentration for exosomes isolated from conditioned media of NT siRNA- and siCALR-treated ZAAT-expressing Huh7.5 cells. The *bold red curves* plot the size distribution of exosomes and show that knocking out calreticulin alters the overall size distribution as well as the mean and concentration. A single population of exosomes purified from NT siRNA-treated cells with a size of 104 nm is shown in the *top graph*. Two distinct populations of exosomes of 84 and 113 nm in size purified from siCALR-treated cells is shown in the *bottom graph*. NanoSight NTA software was used to track particles in Brownian motion. Individual size distribution profiles of three captures for each sample was overplotted. The concentration given under the graphs reflects the actual concentration of exosomes particles per ml after applying the dilution factor (1:1000) for each sample. *D*, Western blotting experiment of the purified exosomes using antibodies to AAT and ERdj3 shows AAT and ERdj3 are present in the siCALR-treated samples at higher concentration. Exosomal markers such as Flotillin-1, annexin A2, and Hsp70 were detectable in the exosome fraction from both NT siRNA and siCALR samples. *E*, quantification of the band intensities of ZAAT and ERdj3 proteins. Differences were assessed by two-tailed *t* test analysis. *, $p < 0.05$. *F*, partial separation of exosomes by optiPrep density gradient shows co-localization of ZAAT and ERdj3 with Alix, CD63, and TSG101in the lower density fractions with the density of 1.069 and 1.079 g/ml. *Lanes 1–8*, respectively, indicate the density of 1.059, 1.069, 1.079, 1.088, 1.112, 1.127, 1.156, and 1.175 g/ml.

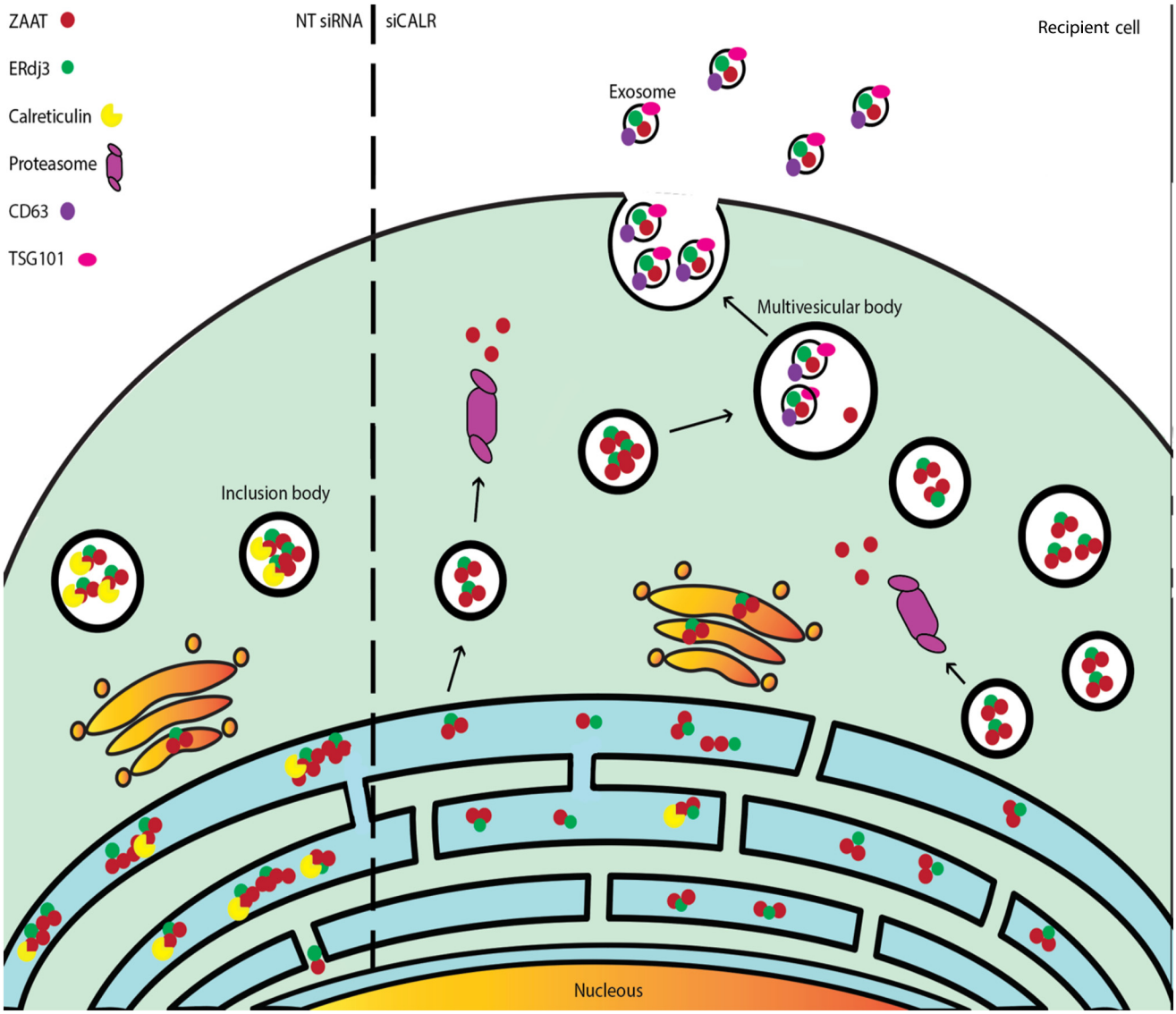

Figure 6. Exosome-mediated ZAAT–ERdj3 secretion. Exosome-mediated ZAAT–ERdj3 secretion is an alternative way for ZAAT degradation when proteasomal degradation machinery is compromised. MVBs are formed by invaginations of late endosomes containing ZAAT–ERdj3 inclusion bodies. Consequently, exosomes are enriched in endosome-associated proteins and ZAAT–ERdj3. These exosomes are secreted by cells by fusion of MVBs with the plasma membrane.

Cell viability assay

Cell viability was determined in the presence of NT siRNA or siCALR using viability/cytotoxicity kit from Invitrogen following the manufacturer's protocol. Briefly, AAT KO Huh 7.5 cells transfected with NT siRNA or siCALR were cultured overnight in a 96-well assay plate. 24 h after silencing, they were transfected with ZAAT plasmid and grown until acceptable cell density. The cells with no treatment were considered a live control, and 0.1% saponin (Sigma) was added to the cells for 10 min for dead cell control. 4 μM of ethidium homodimer-1 and 2 mM of calcein AM were added to each well. The plate was incubated at room temperature for 45 min. Absorbance at 530 and 645 nm was measured and recorded using a microplate reader (6).

Quantitative real-time PCR

Total RNA was extracted from selected cell lines, and the first complementary strand was generated using SuperScript VILO kit from Invitrogen. Expression level of gene products were analyzed by quantitative real-time PCR using an Applied Biosystems 7500 fast real-time PCR system from Life Technologies and TaqMan Universal PCR Master Mix from Roche Applied Science. Pairs of genes were analyzed simultaneously with h18S rRNA used as an endogenous control. The specificity of the priming and amplification was verified with a melt curve for each amplicon. The quantitative real-time PCR was performed in duplicate, and the results were averaged. The results are presented as the relative quantification as determined by the $2^{-\Delta\Delta Ct}$ equation (47).

Metabolic labeling pulse–chase study

Nearly confluent monolayers of AAT knockout Huh 7.5 cells and K41 and K42 cell lines were transfected with/without NT siRNA or siCALR. 24 h after silencing, ZAAT expression vector was introduced into 35-mm-diameter culture dishes. The cells

were incubated for 10 min with [^{35}S]methionine (200–500 mCi/ml of medium; PerkinElmer Life Sciences) (48) and then chased for 40 min by incubation in 1 ml of Dulbecco's modified Eagle's medium/F-12 with 10% fetal bovine serum containing a 5-fold excess of unlabeled methionine. The cells were harvested in a total volume of 500 μl of IP lysis buffer (Pierce), kept on ice, and centrifuged at 15,000 $\times$ *g* for 5 min at 4 °C to precipitate cell debris. ZAAT was immune precipitated from the cell lysate and medium using rabbit anti-human AAT antibody bound to protein A Dyna beads. Immunocomplexes were washed, suspended in 20 μl of sample buffer, heated at 70 °C for 10 min, and analyzed using SDS Tris glycine 10% SDS-PAGE (Bio-Rad). Radiolabeled AAT was detected by autoradiography.

Opti-Prep density gradient isolation of cellular proteins

AAT knockout Huh 7.5 cells were transfected with NT siRNA or 20 nM of siCALR. 24 h after silencing, the cells were transiently transfected with ZAAT. 48 h after transfection with ZAAT, the cells were incubated with or without 20 μM brefeldin A (Sigma) for 6 h and were washed with 1× PBS to remove media and debris. Next, 2 ml of cold isotonic buffer (250 mM sucrose, 1 mM TEA_AC, 1 mM EDTA) was added to 10-cm dishes on ice, and cells were scraped into the buffer, transferred to a 15-ml tube, and then centrifuged at 15,000 $\times$ *g* for 5 min. The pellet was suspended and homogenized in 300 μl of hypotonic buffer (80 mM sucrose, 10 mM TEA_AC, 1 mM EDTA) and 100× Halt protease inhibitor mixture and diluted in 300 μl of hypertonic buffer (420 mM sucrose, 10 mM TEA_AC, 1 mM EDTA). The cell lysate was centrifuged at 3,000 $\times$ *g* for 5 min, and the supernatant was collected and inserted into the step gradient composed of 2.5–30% iodaxanol solutions in 14-ml ultra-clear tubes (Beckman Coulter, Brea, CA). Then within 1 h the tubes were ultra-centrifuged at 90,000 $\times$ *g* for 1 h at 4 °C (SW40Ti rotor, Beckman Coulter). After centrifugation, 11 fractions were collected and stored at −20 °C until analysis.

Immunoblotting and immunoprecipitation

AAT knockout Huh 7.5, K41 and K42 cell lines were seeded at 3 $\times$ 10^5/well in 6-well plates with NT siRNA or siCALR. 24 h after silencing, the cells were transfected with ZAAT plasmid and were collected after 48 h. RIPA or IP lysis buffer was used to lyse the cells. Protein levels in the cell lysate homogenates were determined using the bicinchoninic acid method (Pierce). Total protein was resolved on tris glycine SDS-PAGE gels (Bio-Rad). The proteins were transferred to nitrocellulose membranes. The blots were incubated with rabbit polyclonal antibodies against calnexin and calreticulin (Stressgen Biotechnologies, San Diego, CA); PDI (Cell Signaling, Danvers, MA); CD81, CD63, TSG101, ALIX, and ERdj3 (Proteintech, Chicago, IL); flotilin-1, annexin A2, and Hsp70 from Abcam (Cambridge, UK); or mouse monoclonal antibodies against BiP from BD Bioscience (San Jose, CA); and actin from Sigma overnight at 4 °C after blocking. Proteins were detected by using a Super Signal West Dura extended duration substrate kit from Thermo Scientific. Western blotting band intensities were quantified using Alpha view software (ProteinSimple, San Jose, CA).

To investigate the interaction of ZAAT with ERdj3, co-IP was performed with polyclonal rabbit antibodies against AAT (Dako, Carpentaria, CA) and ERdj3 (Proteintech). The lysates were incubated with anti–AAT-conjugated beads (Life Technologies) overnight at 4 °C. The next day, the beads were washed several times, then suspended in gel loading buffer, and evaluated by Western blotting using antibodies against ERdj3.

Immunostaining and immunofluorescence microscopy

NT siRNA- or siCALR-treated AAT knockout Huh 7.5 cells were grown on glass coverslips and transfected with ZAAT and with or without GFP-Q79L-Rab5 (AddGene) plasmids. 48 h post-transfection, the cells were fixed with 4% paraformaldehyde in PBS for 20 min. The coverslips were washed with 1× PBS. The cells were incubated for 1 h with blocking buffer (1× PBS, 5% goat serum, 0.3% Triton X-100) at room temperature, followed by incubating overnight at 4 °C with primary antibodies (1:400). The cells were washed with 1× PBS and incubated for 1 h with secondary antibodies (Alexa Fluor 488 goat anti-mouse IgG and Alexa Fluor 594 goat anti-rabbit IgG). The coverslips were mounted and sealed. Images were collected using a fluorescence microscope (Nikon, Melville, NY). Samples were scanned with a 0.1-mm step. Images were processed for brightness and contrast and filtered for noise with Volocity 6.3 software (PerkinElmer Life Sciences) following good practices as outlined by Rossner and Yamada (49).

Exosome isolation from cell-conditioned media and characterization

A total of three exosome preparations were performed from consecutive passages of Huh 7.5, K41 and K42 cells. The cells were grown to confluence and then maintained in culture following the treatments with NT siRNA or siCALR for 4 days before the conditioned media were collected. The individual collections of conditioned media from the cells were pooled. Conditioned media were centrifuged at 1,000 $\times$ *g* for 10 min to remove dead cells and cellular debris. The supernatants were collected and filtered with a 0.22-μm (220 nm) Nalgene filter (Thermo Scientific). The resulting supernatant was subjected to centrifugation at 10,000 $\times$ *g* for 30 min to remove any remaining debris and then ultra-centrifuged at 118,000 $\times$ *g* for 70 min at 4 °C with a fixed-angle rotor Ti-70 (Beckman Coulter, Brea, CA). The pellets were washed with sterile 1× PBS and subjected to another cycle of ultracentrifugation at 118,000 $\times$ *g* for 70 min at 4 °C. The supernatant was discarded, and the pelleted exosomes were carefully reconstituted in sterile 1× PBS or lysed in RIPA buffer (both from Thermo Fisher Scientific). Exosome concentration and characterization were determined using NanoSight-based exosome characterization. Floatation Opti-Prep gradient method was performed on the exosome fraction to separate ZAAT aggregates from the exosome vesicles. Exosome morphology was characterized by imaging on a HITACHI 7600 transmission electron microscope equipped with AMTV600 camera at the University of Florida transmission electron microscopy core.

Statistical analysis

All results are expressed as means ± S.E. Statistical analyses were performed using Prism 7 software program (GraphPad

Software) by Student's *t* test or Mann–Whitney *U* test. Values of $p < 0.05$ were considered statistically significant.

Author contributions—N. K. and M. B. conceptualization; N. K., L. S. H., and K. K. data curation; N. K. software; N. K. formal analysis; N. K. and M. B. supervision; N. K. validation; N. K., R. O., and L. S. H. investigation; N. K. visualization; N. K., R. O., A. A. A., K. M. T., and K. K. methodology; N. K. writing-original draft; N. K. and M. B. project administration; R. O., A. A. A., L. S. H., and M. B. writing-review and editing; M. B. resources; M. B. funding acquisition.

Acknowledgments—We thank William A. Dunn for advice and suggestions on this work, Marek Michalak for providing K41 and K42 cell lines, and members of our laboratories for contributions to various aspects of our research. The ultrastructural studies were conducted at the University of Florida College of Medicine Electron Microscopy Core Facility under the kindly supervision of Dr. Jill Verlander, with the assistance of Dr. Sharon Matthews.

References

1. Gooptu, B., Dickens, J. A., and Lomas, D. A. (2014) The molecular and cellular pathology of α_1-antitrypsin deficiency. *Trends Mol. Med.* **20,** 116–127 CrossRef Medline
2. Bals, R. (2010) α_1-Antitrypsin deficiency. *Best Pract. Res. Clin. Gastroenterol.* **24,** 629–633 CrossRef Medline
3. Fregonese, L., and Stolk, J. (2008) Hereditary α_1-antitrypsin deficiency and its clinical consequences. *Orphanet J. Rare Dis.* **3,** 16 CrossRef Medline
4. Greene, C. M., and McElvaney, N. G. (2010) Z α_1-antitrypsin deficiency and the endoplasmic reticulum stress response. *World J. Gastrointest. Pharmacol. Ther.* **1,** 94–101 CrossRef Medline
5. Cabral, C. M., Liu, Y., Moremen, K. W., and Sifers, R. N. (2002) Organizational diversity among distinct glycoprotein endoplasmic reticulum-associated degradation programs. *Mol. Biol. Cell* **13,** 2639–2650 CrossRef Medline
6. Khodayari, N., Marek, G., Lu, Y., Krotova, K., Wang, R. L., and Brantly, M. (2017) Erdj3 has an essential role for Z variant α_1-antitrypsin degradation. *J. Cell. Biochem.* **118,** 3090–3101 CrossRef Medline
7. Sifers, R. N. (2010) Intracellular processing of α_1-antitrypsin. *Proc. Am. Thorac. Soc.* **7,** 376–380 CrossRef Medline
8. Burrows, J. A., Willis, L. K., and Perlmutter, D. H. (2000) Chemical chaperones mediate increased secretion of mutant α_1-antitrypsin (α_1-AT) Z: A potential pharmacological strategy for prevention of liver injury and emphysema in α_1-AT deficiency. *Proc. Natl. Acad. Sci. U.S.A.* **97,** 1796–1801 CrossRef Medline
9. Rabouille, C. (2017) Pathways of unconventional protein secretion. *Trends Cell Biol.* **27,** 230–240 CrossRef Medline
10. Baixauli, F., López-Otín, C., and Mittelbrunn, M. (2014) Exosomes and autophagy: coordinated mechanisms for the maintenance of cellular fitness. *Front. Immunol.* **5,** 403 Medline
11. Mohamed, N. V., Herrou, T., Plouffe, V., Piperno, N., and Leclerc, N. (2013) Spreading of Tau pathology in Alzheimer's disease by cell-to-cell transmission. *Eur. J. Neurosci.* **37,** 1939–1948 CrossRef Medline
12. Lee, J. G., Takahama, S., Zhang, G., Tomarev, S. I., and Ye, Y. (2016) Unconventional secretion of misfolded proteins promotes adaptation to proteasome dysfunction in mammalian cells. *Nat. Cell Biol.* **18,** 765–776 CrossRef Medline
13. Saman, S., Kim, W., Raya, M., Visnick, Y., Miro, S., Saman, S., Jackson, B., McKee, A. C., Alvarez, V. E., Lee, N. C., and Hall, G. F. (2012) Exosome-associated Tau is secreted in tauopathy models and is selectively phosphorylated in cerebrospinal fluid in early Alzheimer disease. *J. Biol. Chem.* **287,** 3842–3849 CrossRef Medline
14. Willms, E., Johansson, H. J., Mäger, I., Lee, Y., Blomberg, K. E., Sadik, M., Alaarg, A., Smith, C. I., Lehtiö, J., El Andaloussi, S., Wood, M. J., and Vader, P. (2016) Cells release subpopulations of exosomes with distinct molecular and biological properties. *Sci. Rep.* **6,** 22519 CrossRef Medline
15. Colombo, M., Raposo, G., and Théry, C. (2014) Biogenesis, secretion, and intercellular interactions of exosomes and other extracellular vesicles. *Annu. Rev. Cell Dev. Biol.* **30,** 255–289 CrossRef Medline
16. Théry, C., Zitvogel, L., and Amigorena, S. (2002) Exosomes: composition, biogenesis and function. *Nat. Rev. Immunol* **2,** 569–579 CrossRef Medline
17. Genereux, J. C., Qu, S., Zhou, M., Ryno, L. M., Wang, S., Shoulders, M. D., Kaufman, R. J., Lasmezas, C. I., Kelly, J. W., and Wiseman, R. L. (2015) Unfolded protein response-induced ERdj3 secretion links ER stress to extracellular proteostasis. *EMBO J.* **34,** 4–19 CrossRef Medline
18. Bergmann, T. J., Fregno, I., Fumagalli, F., Rinaldi, A., Bertoni, F., Boersema, P. J., Picotti, P., and Molinari, M. (2018) Chemical stresses fail to mimic the unfolded protein response resulting from luminal load with unfolded polypeptides. *J. Biol. Chem.* **293,** 5600–5612 CrossRef Medline
19. Mesaeli, N., Nakamura, K., Zvaritch, E., Dickie, P., Dziak, E., Krause, K. H., Opas, M., MacLennan, D. H., and Michalak, M. (1999) Calreticulin is essential for cardiac development. *J. Cell Biol.* **144,** 857–868 CrossRef Medline
20. Fra, A., Cosmi, F., Ordoñez, A., Berardelli, R., Perez, J., Guadagno, N. A., Corda, L., Marciniak, S. J., Lomas, D. A., and Miranda, E. (2016) Polymers of Z α_1-antitrypsin are secreted in cell models of disease. *Eur. Respir. J.* **47,** 1005–1009 CrossRef Medline
21. Takeuchi, T., Suzuki, M., Fujikake, N., Popiel, H. A., Kikuchi, H., Futaki, S., Wada, K., and Nagai, Y. (2015) Intercellular chaperone transmission via exosomes contributes to maintenance of protein homeostasis at the organismal level. *Proc. Natl. Acad. Sci. U.S.A.* **112,** E2497–E2506 CrossRef Medline
22. Dang, V. D., Jella, K. K., Ragheb, R. R. T., Denslow, N. D., and Alli, A. A. (2017) Lipidomic and proteomic analysis of exosomes from mouse cortical collecting duct cells. *FASEB J.* **31,** 5399–5408 CrossRef Medline
23. Aalberts, M., van Dissel-Emiliani, F. M., van Adrichem, N. P., van Wijnen, M., Wauben, M. H., Stout, T. A., and Stoorvogel, W. (2012) Identification of distinct populations of prostasomes that differentially express prostate stem cell antigen, annexin A1, and GLIPR2 in humans. *Biol. Reprod.* **86,** 82 Medline
24. Bobrie, A., Colombo, M., Krumeich, S., Raposo, G., and Thery, C. (2012) Diverse subpopulations of vesicles secreted by different intracellular mechanisms are present in exosome preparations obtained by differential ultracentrifugation. *J. Extracell. Vesicles* **1,** 18397 CrossRef Medline
25. Roberts, R. L., Barbieri, M. A., Pryse, K. M., Chua, M., Morisaki, J. H., and Stahl, P. D. (1999) Endosome fusion in living cells overexpressing GFP-rab5. *J. Cell Sci.* **112,** 3667–3675 Medline
26. Pols, M. S., and Klumperman, J. (2009) Trafficking and function of the tetraspanin CD63. *Exp. Cell Res.* **315,** 1584–1592 CrossRef Medline
27. Wyatt, A. R., Yerbury, J. J., Ecroyd, H., and Wilson, M. R. (2013) Extracellular chaperones and proteostasis. *Annu. Rev. Biochem.* **82,** 295–322 CrossRef Medline
28. Wyatt, A. R., Yerbury, J. J., Dabbs, R. A., and Wilson, M. R. (2012) Roles of extracellular chaperones in amyloidosis. *J. Mol. Biol.* **421,** 499–516 CrossRef Medline
29. Genereux, J. C., and Wiseman, R. L. (2015) Regulating extracellular proteostasis capacity through the unfolded protein response. *Prion* **9,** 10–21 CrossRef Medline
30. Tan, Y. L., Genereux, J. C., Pankow, S., Aerts, J. M., Yates, J. R., 3rd, Kelly, J. W. (2014) ERdj3 is an endoplasmic reticulum degradation factor for mutant glucocerebrosidase variants linked to Gaucher's disease. *Chem. Biol.* **21,** 967–976 CrossRef Medline
31. Shen, Y., and Hendershot, L. M. (2005) ERdj3, a stress-inducible endoplasmic reticulum DnaJ homologue, serves as a cofactor for BiP's interactions with unfolded substrates. *Mol. Biol. Cell* **16,** 40–50 CrossRef Medline
32. Caramelo, J. J., and Parodi, A. J. (2008) Getting in and out from calnexin/calreticulin cycles. *J. Biol. Chem.* **283,** 10221–10225 CrossRef Medline
33. Teckman, J. H., Burrows, J., Hidvegi, T., Schmidt, B., Hale, P. D., and Perlmutter, D. H. (2001) The proteasome participates in degradation of mutant α_1-antitrypsin Z in the endoplasmic reticulum of hepatoma-derived hepatocytes. *J. Biol. Chem.* **276,** 44865–44872 CrossRef Medline
34. Eitan, E., Suire, C., Zhang, S., and Mattson, M. P. (2016) Impact of lysosome status on extracellular vesicle content and release. *Ageing Res. Rev.* **32,** 65–74 CrossRef Medline

35. Palma, J., Yaddanapudi, S. C., Pigati, L., Havens, M. A., Jeong, S., Weiner, G. A., Weimer, K. M., Stern, B., Hastings, M. L., and Duelli, D. M. (2012) MicroRNAs are exported from malignant cells in customized particles. *Nucleic Acids Res.* **40,** 9125–9138 CrossRef Medline
36. Zomer, A., Vendrig, T., Hopmans, E. S., van Eijndhoven, M., Middeldorp, J. M., and Pegtel, D. M. (2010) Exosomes: fit to deliver small RNA. *Commun. Integr. Biol.* **3,** 447–450 CrossRef Medline
37. Pegtel, D. M., Cosmopoulos, K., Thorley-Lawson, D. A., van Eijndhoven, M. A., Hopmans, E. S., Lindenberg, J. L., de Gruijl, T. D., Würdinger, T., and Middeldorp, J. M. (2010) Functional delivery of viral miRNAs via exosomes. *Proc. Natl. Acad. Sci. U.S.A.* **107,** 6328–6333 CrossRef Medline
38. Stoorvogel, W., Kleijmeer, M. J., Geuze, H. J., and Raposo, G. (2002) The biogenesis and functions of exosomes. *Traffic* **3,** 321–330 CrossRef Medline
39. de Gassart, A., Geminard, C., Fevrier, B., Raposo, G., and Vidal, M. (2003) Lipid raft-associated protein sorting in exosomes. *Blood* **102,** 4336–4344 CrossRef Medline
40. Meister, M., and Tikkanen, R. (2014) Endocytic trafficking of membrane-bound cargo: a flotillin point of view. *Membranes* **4,** 356–371 CrossRef Medline
41. Phuyal, S., Hessvik, N. P., Skotland, T., Sandvig, K., and Llorente, A. (2014) Regulation of exosome release by glycosphingolipids and flotillins. *FEBS J.* **281,** 2214–2227 CrossRef Medline
42. Hunziker, W., Whitney, J. A., and Mellman, I. (1992) Brefeldin A and the endocytic pathway. Possible implications for membrane traffic and sorting. *FEBS Lett.* **307,** 93–96 CrossRef Medline
43. Nebenführ, A., Ritzenthaler, C., and Robinson, D. G. (2002) Brefeldin A: deciphering an enigmatic inhibitor of secretion. *Plant Physiol.* **130,** 1102–1108 CrossRef Medline
44. Wood, S. A., Park, J. E., and Brown, W. J. (1991) Brefeldin A causes a microtubule-mediated fusion of the trans-Golgi network and early endosomes. *Cell* **67,** 591–600 CrossRef Medline
45. Février, B., and Raposo, G. (2004) Exosomes: endosomal-derived vesicles shipping extracellular messages. *Curr. Opin. Cell Biol.* **16,** 415–421 CrossRef Medline
46. Fairbanks, K. D., and Tavill, A. S. (2008) Liver disease in α_1-antitrypsin deficiency: a review. *Am. J. Gastroenterol.* **103,** 2136–2142 CrossRef Medline
47. Khodayari, N., Wang, R. L., Marek, G., Krotova, K., Kirst, M., Liu, C., Rouhani, F., and Brantly, M. (2017) SVIP regulates Z variant α_1-antitrypsin retro-translocation by inhibiting ubiquitin ligase gp78. *PLoS One* **12,** e0172983 CrossRef Medline
48. Novoradovskaya, N., Lee, J., Yu, Z. X., Ferrans, V. J., and Brantly, M. (1998) Inhibition of intracellular degradation increases secretion of a mutant form of α_1-antitrypsin associated with profound deficiency. *J. Clin. Invest.* **101,** 2693–2701 CrossRef Medline
49. Rossner, M., and Yamada, K. M. (2004) What's in a picture? The temptation of image manipulation. *J. Cell Biol.* **166,** 11–15 CrossRef Medline